processes

MDPI

Article

Impact of the UV/H_2O_2 Process on Assimilable Organic Carbon and Trihalomethane Formation in Cyanobacteria-Contaminated Waters

Luciana Verissimo Siquerolo [1], Rúbia Martins Bernardes Ramos [1], Pablo Inocêncio Monteiro [2], Guilherme Ferreira Silveira [3], Fatima de Jesus Bassetti [1] and Lucila Adriani de Almeida Coral [1,*]

[1] Posgraduate Program in Environmental Science and Technology, Federal University of Technology—Paraná (UTFPR), R. Deputado Heitor Alencar Furtado, 5000—CIC, Curitiba 81280-340, PR, Brazil; licenzasa@gmail.com (L.V.S.); rubiaramos@utfpr.edu.br (R.M.B.R.); bassetti@utfpr.edu.br (F.d.J.B.)
[2] Posgraduate Program in Food Engineering, Chemical Engineering Department, Federal University of Parana, Curitiba 81531-980, PR, Brazil; pabloinocencio@ufpr.br
[3] Oswaldo Cruz Foundation, Carlos Chagas Institute, Curitiba 81350-010, PR, Brazil; gfsilveira@gmail.com
* Correspondence: lucilacoral@utfpr.edu.br

Abstract: The organic material from cyanobacteria is a significant precursor to the generation of disinfection byproducts. This study's aim was to evaluate the formation of assimilable organic carbon (AOC) in water contaminated with cyanobacteria. Furthermore, the formation of AOC was related to the generation of trihalomethanes (THMs) and dissolved organic carbon (DOC). The advanced oxidation process was caISOrried out by exposing Microcystis aeruginosa cells (250,000 cells mL^{-1}) to different peroxide dosages (10 to 100 mg L^{-1}) under ultraviolet radiation. *Pseudomonas fluorescens* (P-17), *Spirillum* sp. (NOX), and flow cytometry were used to determine the AOC concentration. The formation of AOC and THMs during the UV/H_2O_2 process was not directly related. The AOC concentration increased with low H_2O_2 doses and decreased at higher concentrations, while the levels of THMs decreased regardless of the AOC formed. After oxidation, the DOC concentration decreased, along with the concentration of THMs. Additionally, it was observed that the behavior of DOC and AOC is inversely proportional. These results suggest that the oxidation process has a complex effect on organic matter, influencing byproduct formation and AOC availability. Moreover, these findings highlight the importance of carefully monitoring and controlling the oxidation processes to better understand their impact on water treatment and byproduct formation.

Keywords: oxidation process; flow cytometry; byproduct formation; water treatment

check for updates

Academic Editors: Jayaprakash Saththasivam and A. M. Mimi Sakinah

Received: 30 November 2024
Revised: 17 December 2024
Accepted: 23 December 2024
Published: 26 December 2024

Citation: Siquerolo, L.V.; Ramos, R.M.B.; Monteiro, P.I.; Silveira, G.F.; Bassetti, F.d.J.; Coral, L.A.d.A. Impact of the UV/H_2O_2 Process on Assimilable Organic Carbon and Trihalomethane Formation in Cyanobacteria-Contaminated Waters. *Processes* **2025**, *13*, 23. https://doi.org/10.3390/pr13010023

Copyright: © 2024 by the authors. Licensee MDPI, Basel, Switzerland. This article is an open access article distributed under the terms and conditions of the Creative Commons Attribution (CC BY) license (https://creativecommons.org/licenses/by/4.0/).

1. Introduction

The growth of cyanobacteria in reservoirs and eutrophic lakes is becoming increasingly prevalent. A previous study [1] predicted that by the mid-21st century, the concentration of cyanobacteria and phytoplankton in lakes is expected to increase due to factors such as land use and climatic conditions. The proliferation of cyanobacteria in water sources used for public supply primarily results in the presence of organic matter derived from their cells [2]. This organic matter serves as a key precursor to disinfection byproducts (DBPs), such as emerging nitrogenous DBPs (N-DBPs), haloacetic acids (HAAs), and total trihalomethanes (THMs). These byproducts are associated with significant genotoxic

and carcinogenic risks [3–5]. In water distribution systems, the most common THMs are bromoform, dibromochloromethane, bromodichloromethane, and chloroform [6].

Given the potential of oxidizing agents for degrading cyanotoxins in water, the use of oxidative processes in treatment is seen as a promising approach to ensuring water quality. However, the application of oxidants and disinfectants in public water treatment leads to the formation of byproducts. One of these byproducts, resulting from the oxidation of organic matter, is assimilable organic carbon (AOC). Its concentration indicates the water's biological stability, reflecting its potential to support heterotrophic microorganism growth [7]. Studies relate AOC with decreased drinking water quality, biofouling, and the growth of microorganisms [8–10]. Additionally, the presence of AOC may contribute to the formation of THMs.

Advanced oxidation processes (AOPs) can be used as a pre-treatment step for contaminated water. AOPs are methods that employ highly reactive species to break down organic substances that are difficult to decompose into simpler compounds [11]. Different compounds can be degraded by AOPs, including pharmaceuticals, antibiotics, herbicides, organic matter [12], and cyanotoxin. Various AOPs, including ozonation [13], UV/$KMnO_4$ systems [14], and Fenton-electrocoagulation systems [15], have shown effectiveness in removing cyanobacteria and their toxins. The UV/H_2O_2 process has also demonstrated efficacy. However, similar to other processes, it can produce precursors to oxidation byproducts, such as AOC.

For this reason, it is fundamental to precisely regulate the operational parameters, such as dosage and contact time, in the UV/H_2O_2 process to ensure its efficiency. This regulation aims to achieve the complete degradation of cyanotoxins and minimize AOC formation. Although it is known that the oxidation of natural organic matter increases AOC concentrations, there are limited data on AOC formation, specifically from cyanobacteria.

Given the increasing presence of cyanobacteria in water sources and the use of oxidative processes in water treatment systems, it is important to understand how these microorganisms can affect the formation of DBPs, THMs, and AOC. This study aims to evaluate the contribution of cyanobacteria to the formation of AOC through the UV/H_2O_2 oxidative process and its influence on the generation of THMs in water samples contaminated with cyanobacteria. Additionally, the relationship between AOC and dissolved organic carbon (DOC), as well as between THMs and DOC, was also analyzed after the advanced oxidative process. This work provides insight into the formation of byproducts and their relevance for application in water treatment processes, particularly in waters contaminated with cyanobacteria.

2. Materials and Methods

2.1. Chemical Reagents

The chemical reagents used were: magnesium sulfate ($MgSO_4$, Synth, Diadema, Brazil, 98%), sodium bicarbonate ($NaHCO_3$, Neon, Suzano, Brazil, 99%), potassium chloride (KCl, Neon, Brazil, 99–100.5%), calcium sulfate dihydrate ($CaSO_4 \cdot 2H_2O$, Reatec, Colombo, Brazil, 98%), hydrogen peroxide (H_2O_2, AppliChem, Darmstadt, Germany, 30%), sodium thiosulfate ($Na_2S_2O_3$, Alphatec, São Bernardo do Campo, Brazil, 99.5–101%), sodium acetate (CH_3COONa, Neon, Brazil, 99.1%), paraformaldehyde ($OH(CH_2O)nH$ (n = 8–100, Dinâmica, Indaiatuba, Brazil, 89–93%)), Potassium biphthalate (Neon, Brazil, 99.63%), potassium iodide (KI, Alphatec, Brazil, 99%), sodium hydroxide (NaOH, Dinâmica, Brazil, 98%), ammonium molybdate tetrahydrate ($(NH_4)_6Mo_7O_{24} \cdot 4H_2O$, Alphatec, Brazil, 99%), free chlorine (Cl_2) (commercial kit, Alfakit, Florianópolis, Brazil), sodium bisulfite ($NaHSO_3$, Neon, Brazil, 66.34%), and R2A agar (EP, USP, Kasvi, Conda S.A., Madrid, Spain). Distilled and ultrapure water was used in the procedures.

2.2. Cyanobacteria Cultivation

To enable the proposed experiments, a toxic strain of the cyanobacterium *Microcystis aeruginosa* was cultured at the Water Treatment and Potabilization Laboratory of Federal University of Technology—Paraná (UTFPR), Curitiba campus, Brazil. The strain was provided by the School of Engineering of São Paulo State University (UNESP) at Ilha Solteira, Brazil. *Microcystis aeruginosa* (toxic strain) was kept in a climate-controlled environment at approximately 26 °C. It was provided with constant aeration and a 16/8 h light/dark photoperiod. The strain was cultured in ASM-1 medium [16] and used during the exponential growth phase, between 20 and 23 days of cultivation.

2.3. Water of the Study

The water used in the study was moderately hard synthetic freshwater, prepared by adding inorganic salts (60.0 mg L^{-1} $MgSO_4$, 96.0 mg L^{-1} $NaHCO_3$, 4.0 mg L^{-1} KCl, and 60.0 mg L^{-1} $CaSO_4 \cdot 2H_2O$) [17], and contaminated with *M. aeruginosa* cells. These cells served as the sole carbon source in the water. This approach ensured that variations in the initial water quality did not interfere with the results throughout the study and allowed for the formation of THMs derived from the organic matter of the cyanobacterial cells. For each water sample, 100 mL of *M. aeruginosa* culture was centrifuged at 4000 rpm for 10 min. The cells were resuspended in synthetic water and then vortexed before being prepared for cell density determination. The volume required to achieve a cell density of 250,000 cells mL^{-1} was determined after cell counting using a Neubauer chamber and optical microscope. The sample was kept at a neutral pH.

2.4. H_2O_2/UV Process

A jacketed glass reactor (0.75 L) was used for the advanced oxidation experiments. A high-pressure mercury lamp (125 W, 254 nm) was placed in a quartz tube, which remained submerged in the sample liquid, allowing uniform irradiation inside the sample. The reactor features a double wall, linking it to a cooling system to prevent overheating of the liquid and the lamp. The reactor was kept under constant agitation using a magnetic stirrer. The photo-oxidative system was installed in a protective wooden box, adapted for electrical installation, with the reactor connected to the lamp and side openings for cables and necessary tubing. The reactor temperature was maintained at 25 ± 1 °C by cooling provided through a thermostatic bath with a recirculation pump.

The samples were collected before the oxidative process and after 90 min of each batch to measure DOC, AOC, THM, and cell count. Before the activation of the UV lamp, hydrogen peroxide (30%) was added in different doses (10, 25, 50, 75, and 100 mg L^{-1}) to the sample. The *M. aeruginosa* cell density used in the study was 250,000 cells mL^{-1}. Tests were carried out to determine the decay of H_2O_2 concentration throughout the oxidative process, in which the total consumption of the oxidizing agent in the medium was determined.

2.5. Determination of Assimilable Organic Carbon (AOC) Concentration

The determination of AOC concentration was carried out using a combined approach based on two methods. The first method uses microorganisms, such as the *Pseudomonas fluorescens* (P-17) (ATCC 9642) and *Spirillum* sp. (NOX) (ATCC 49643) strains, for AOC quantification through plate counting [18], while the second method employs flow cytometry for cell counting [19]. The cell counting in this study was performed using flow cytometry to reduce testing time and adopt a more reliable counting method with fewer errors compared to plate counting. The bacterial strains P-17 and NOX were used in this phase. The equipment used for cell counting of the P-17 and NOX strains was a flow cytometer from Becton and Dickinson, model FACSCanto™ II (Franklin Lakes, NJ, USA).

The cytometer was equipped with 488, 405, and 640 nm lasers and utilized FSC (for cell size) and SSC (for cell complexity) filters with 488/10 and 488/10 configurations.

All materials and glassware used for AOC determination were prepared to be carbon-free. The glassware and materials were washed with neutral detergent and rinsed with water. They were then immersed in 0.1 M HCl for 60 min. After this, they were rinsed three times with ultrapure water. Once dried at room temperature, the materials were wrapped in laminated paper and placed in a muffle furnace (660 °C for 6 h). All materials that could not be placed in the muffle furnace were immersed for 60 min at 60 °C in a 10% (*w*/*v*) sodium persulfate solution and rinsed three times. Ultrapure water was used during this step.

2.5.1. Determination of the Stationary Growth Phase of P-17 and NOX Microorganisms

Before inoculum preparation, *Pseudomonas fluorescens* P-17 (ATCC 9642) and *Spirillum* sp. NOX (ATCC 49643) strains, purchased from the American Type Culture Collection, were activated by inoculation in nutrient agar medium in Petri dishes and kept in a bacteriological incubator at 25 °C. Between 24 and 48 h and approximately six days, strains P-17 and NOX, respectively, were inoculated in inclined tubes with R2 agar. The tubes were kept in an incubator at 25 °C until the growth time for each strain was reached and were then stored under refrigeration for later use.

The individual suspension of each microorganism (P-17 and NOX) was prepared as follows: In each tube containing the pure cultures in inclined R2 agar medium, 2 to 3 mL of ultrapure water was added. To neutralize the residual chlorine in the ultrapure water, it was autoclaved, filtered with a syringe filter (0.22 µm polyethersulfone filter), and supplemented with 45 µL of sodium thiosulfate for every 50 mL of sample. The tubes were then shaken to transfer the colonies from the agar to the water. From this suspension, 100 µL of each culture was transferred to 50 mL of filtered distilled water (individual flasks). To the flasks containing 50 mL of water, 125 µL of sodium acetate (400 mg of acetate-C L^{-1}) was added as a carbon source so that the suspension would present a concentration of 1 mg of acetate-C L^{-1}. A bacteriological incubator was used to incubate the samples at 25 °C until they reached a steady state [18]. The steady state was determined by the growth kinetics of the strains over 120 h. Aliquots were taken from the flasks with individual suspensions at 0, 24, 48, 72, 96, and 120 h. Paraformaldehyde (1.5%) was used to preserve the samples at low temperature. Flow cytometry was employed for cell quantification.

2.5.2. Preparation of Samples for AOC Quantification

For sample preparation, 50 mL aliquots were collected before and after the UV/H_2O_2 process, and 3.3 µL of sodium thiosulfate was added to the aliquots. This addition was necessary to inactivate the chlorine present in the water. Then, the samples were filtered through 0.22 µm polyethersulfone syringe filters. After filtration, they were pasteurized at 70 °C for 60 min. Pasteurization was performed to inactivate the microorganisms present in the sample [19]. After the thermal treatment, the samples were cooled and inoculated with the individual suspension of each strain (P-17 and NOX). The cell density at this stage was 1.10×10^6 cells mL^{-1}. Next, the samples were incubated (96 h at 25 °C) until they reached the stationary phase. Afterwards, the samples were preserved with paraformaldehyde and kept at low temperatures until quantification by flow cytometry.

The number of cells present in the sample was calculated based on Equation (1) [19,20]:

$$\text{AOC } (\mu\text{gC L}^{-1}) = \frac{\text{Cell growth } (\text{L}^{-1})}{1 \times 10^7 \ (\text{Cells}\cdot\mu\text{g L}^{-1})} \quad (1)$$

where AOC is the assimilable organic carbon (μgC L^{-1}), and the bacterial cell concentration in the stationary phase is associated with the consumed AOC, based on the conversion where 1 μg of AOC is equivalent to 1×10^7 cells, as proposed in a previous study [17,18]. The net cell density was determined as the difference between the cell density measured in the stationary phase and the density immediately after inoculation. This net cell density was then converted to carbon equivalents (μgC L^{-1}) using Equation (1) [21].

2.5.3. Effect of Bisulfite as a Hydrogen Peroxide Scavenging Agent on the Quantification of AOC

The effect of sodium bisulfite ($NaHSO_3$), a chemical compound that neutralizes the action of H_2O_2, was evaluated in this study. Neutralizing H_2O_2 is necessary due to its ability to inhibit microorganism growth that can lead to inaccurate AOC quantification if residual concentrations above 0.2 ppm remain in the samples. However, sodium bisulfite can have antimicrobial effects, interfering with the growth of microorganisms (P-17 and NOX) used for AOC quantification. Therefore, sodium bisulfite interference on microorganism growth was assessed by comparing samples with and without the reagent to determine if it would impact AOC quantification.

A 100 mg L^{-1} hydrogen peroxide solution was used to oxidize a 750 mL sample of study water in the UV reactor for 90 min. After the reaction, 50 mL of treated water was supplemented with bisulfite. The samples were filtered (0.22 μm), pasteurized (70 °C for 30 min), and individually incubated (100 μL of P-17 and NOX inoculums at 25 °C for 96 h). After reaching a stationary phase, samples were analyzed using flow cytometry. Initial cell densities were not the same for P-17 and NOX cultures, which could result in differences in the initial cell concentration between the cultures.

2.6. Quantification of Hydrogen Peroxide Residual

The residual H_2O_2 concentration was measured by the reaction with iodide catalyzed by ammonium molybdate [22,23]. Two solutions were prepared for addition to the samples: solution A (potassium hydrogen phthalate + distilled water) and solution B (potassium iodide + sodium hydroxide + ammonium molybdate tetrahydrate + distilled water). To each sample, 2.5 mL of solution A, 2.5 mL of solution B, and 0.5 mL of study water diluted with distilled water in a 10 mL volumetric flask were added. The blank sample consisted of 2.5 mL of solutions A and B, diluted with distilled water in a 10 mL volumetric flask, while the zero sample was prepared with distilled water. After preparation, the samples were analyzed using a spectrophotometer at 351 nm.

The following equation was used to calculate the residual H_2O_2:

$$[H_2O_2]\ (\text{ppm}) = \frac{(\text{Abs sample} - \text{Abs blank}) \times 10 \times \text{D}}{(0.7776 \times \text{S})} \quad (2)$$

where D is the additional dilution and S is sample volume (0.5 mL). The concentration of hydrogen peroxide (ppm) is determined using Equation (2), which calculates the absorbance difference between the sample and the blank, with adjustments for potential dilutions and the characteristics of the measurement system.

2.7. Determination of Dissolved Organic Carbon (DOC) Level

For DOC level determination, samples were filtered using cellulose acetate membranes with a pore size of 0.45 μm. The samples were then acidified (pH < 2.0). The analysis was performed using the Thermo HiperTOC (Thermo Scientific, Cambridge, UK) analyzer, following the combustion method at 680 °C for CO_2 detection [18].

2.8. Determination of Trihalomethanes (THMs) Level

For THM level determination, the samples were subjected to chlorination. Chlorination allows the formation of disinfection byproducts. Chlorine was added until the residual free chlorine concentration reached 1 ± 0.2 mg L^{-1} (after 24 h, 25 °C). For chlorine analysis, the Spectro Chlorine DPD Free kit (Alfakit, cod. 204) was used with a spectrophotometer (515 nm) [18]. After chlorination, the samples were transferred to 40 mL vials (bubble-free). To these samples, 100 µL of HCl 1:1 was added, and the samples were stored under refrigeration at 5 °C.

Gas chromatography was used for the determination of THMs level. The chromatograph used was the Agilent (Santa Clara, CA, USA), equipped with a triple quadrupole mass spectrometry detector and a chromatographic column with a stationary phase composed of 6% Cyanopropyl and 94% Dimethylpolysiloxane. The column had a film thickness of 1.4 µm, a diameter of 0.25 mm, and a length of 60 m. The system also included helium and nitrogen gases and an automatic injection system, CombiPAL. This methodology allowed for the quantification of the trihalomethanes bromoform, dibromochloromethane, bromodichloromethane, and chloroform.

3. Results and Discussions

3.1. Flow Cytometry Counting

Figure 1 shows the flow cytometry cell count of P-17 and NOX microorganisms in the liquid medium. The counts showed that distinguishing the two cell types was not possible when the strains were inoculated concomitantly in the liquid medium. Both strains occupy the same reading region. This suggests that they have similar cell complexity and size, preventing their differentiation at the cytometry level. Although it did not allow differentiation of the microorganisms, it provides more stable data than plating, which can be more susceptible to bacterial physiological changes or human error.

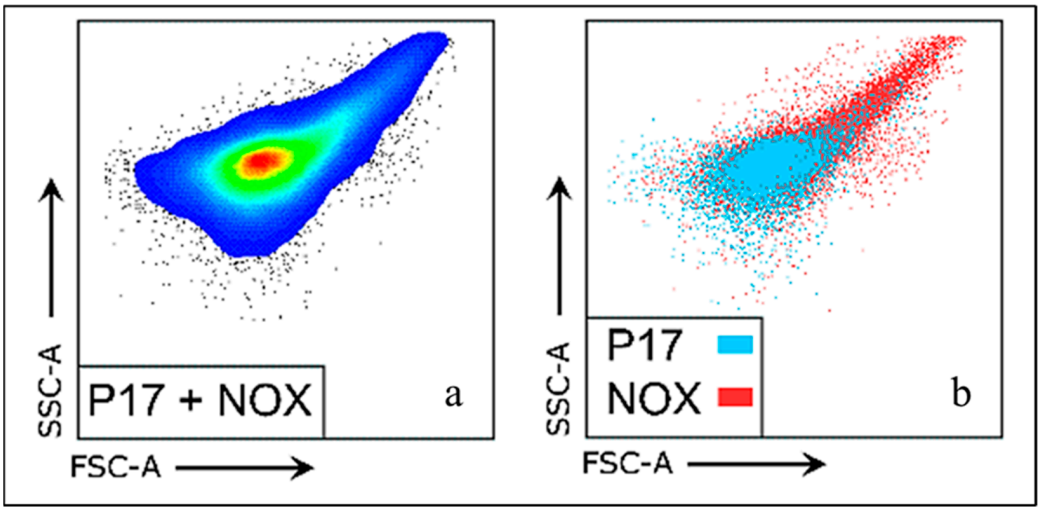


Figure 1. Flow cytometry representing the cell count of the microorganisms P-17 and NOX in liquid medium; area of highest population density (red, yellow, and green); area of lowest population density (light blue and dark blue). (**a**) Density plot; (**b**) Dot plot (FSC-A—Cell size, SSC-A—cell complexity).

Additionally, flow cytometry can be performed with precision and high speed [19], making it a more efficient method for quantification. However, strain differentiation during cell counting is important for evaluating the AOC quantification for each microorganism. It allows measuring the amount of AOC from the growth of the P-17 and NOX strains. To achieve this, the microorganisms were inoculated separately in this study. This was

possible due to their consumption of different carbon sources: for P-17, carbohydrates and amino acids, and for NOX, oxalic acid and carboxylic acids. The separation did not interfere with the AOC quantification, as there was no competition for carbon. For the next steps of this study, AOC quantification was performed separately for each strain, and the concentrations were summed to obtain the total AOC value in the samples.

3.2. Definition of the Stationary Phase of P-17 and NOX

The growth kinetics of the P-17 and NOX strains allowed for the determination of the time required for each strain to reach the stationary phase. Figure 2 shows the cell growth data collected over 168 h of incubation. The stationary phase is reached when the cell density no longer increases. At 25 °C, both strains entered the stationary phase between 72 and 96 h. Based on the results, it was considered that the number of microorganisms at these hours represents the maximum cell count that the carbon source in the sample can sustain.

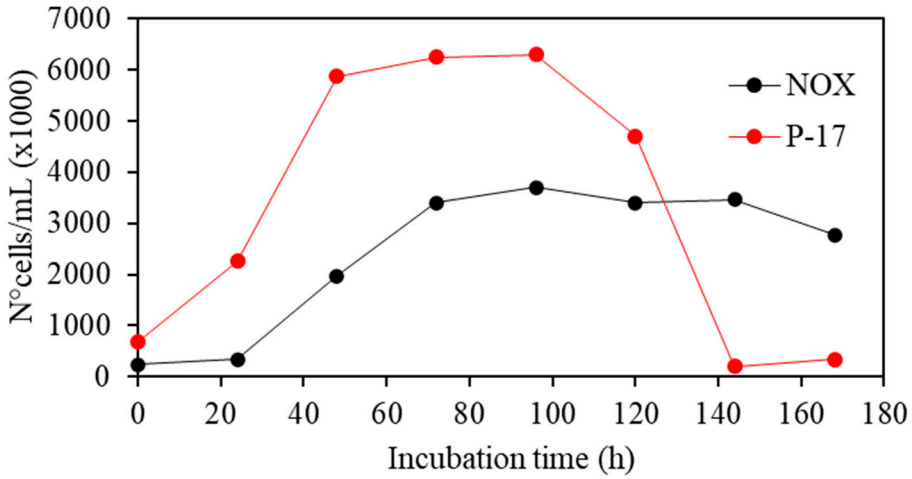


Figure 2. Growth curve of microorganisms P-17 and NOX.

3.3. Evaluation of the Interference of Sodium Bisulfite on the Growth of P-17 and NOX

Figure 3 shows the flow cytometry graphs (density plots) related to the cell density measurements under the evaluated conditions (initial sample, without sodium bisulfite, and with sodium bisulfite). It is observed that both P-17 and NOX cultures were affected by sodium bisulfite, which interfered with their growth. The cell grouping in the graphs suggests the presence of P-17 and NOX populations with similar cellular morphology. The greater the distance of a population from the central grouping, the larger the difference in terms of cellular complexity and size. In the NOX samples, the bisulfite resulted in limited growth of the microorganisms. On the other hand, the bisulfite acted as an antimicrobial agent and inhibited microbial growth in the P-17 sample. A previous study [24] used immobilized bovine catalase to remove hydrogen peroxide (H_2O_2) in AOC analyses. Although bovine catalase is effective, it is expensive. Therefore, this study decided not to use chemical agents to remove H_2O_2, aiming to reduce costs and avoid inhibiting microbial growth. Alternatively, it was essential to assess the H_2O_2 degradation time under UV light to ensure complete consumption of H_2O_2 by the end of the reaction, enabling precise AOC quantification without any residual H_2O_2.

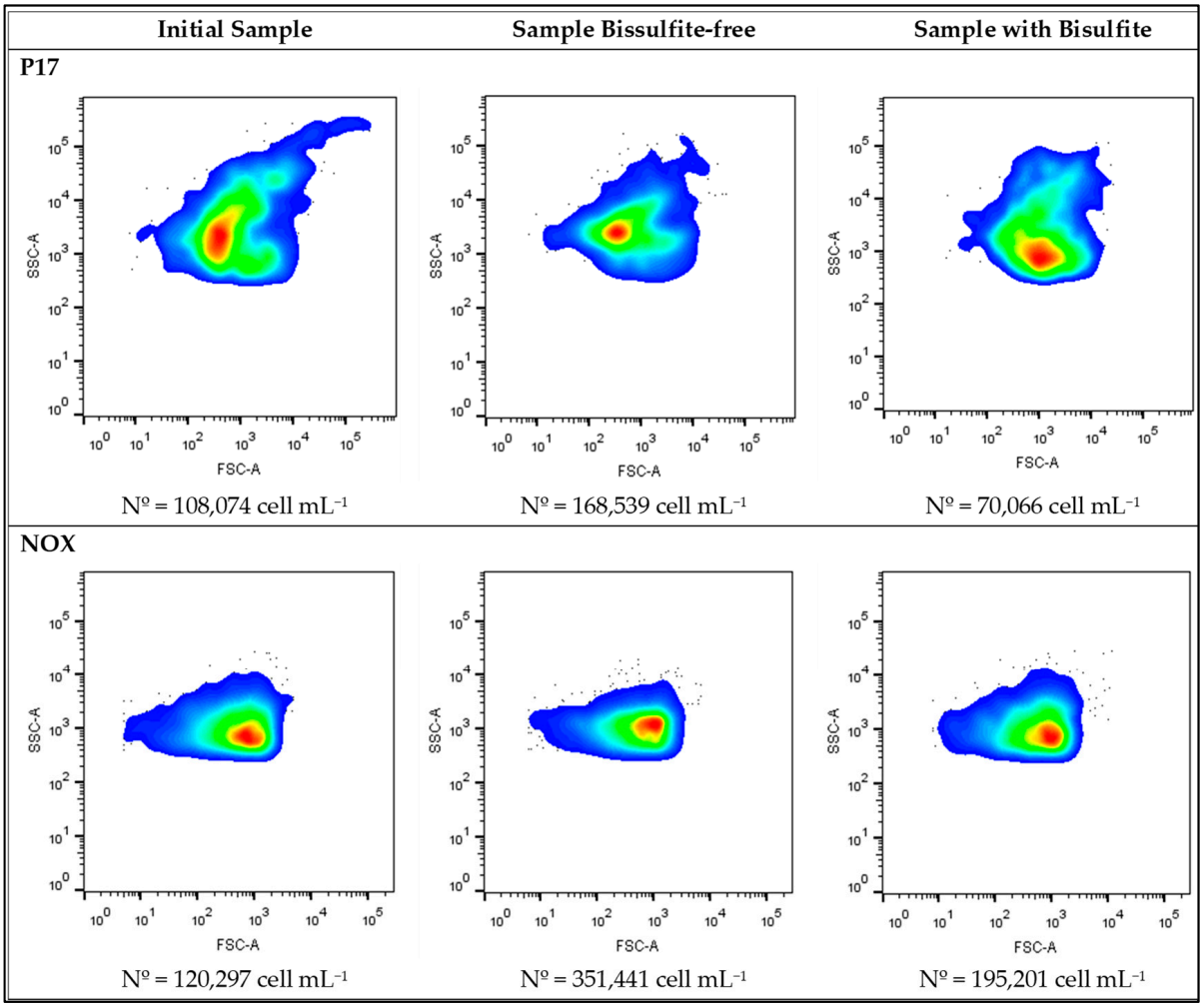


Figure 3. Cell density of microorganisms in the presence and absence of sodium bisulfite through the flow cytometry "density plot" graph. The warm colors (red, yellow, and green) represent areas of higher population density; the cool colors (light blue and dark blue) indicate areas of lower density (After 96 h of growth); FSC-A (cell size); SSC-A (cellular complexity).

3.4. Estimation of UV Exposure Time for Hydrogen Peroxide Degradation

Figure 4 shows the degradation curve of peroxide concentration under UV light exposure. After 30 min of reaction, complete peroxide degradation was achieved for the 10 and 25 mg L^{-1} doses. However, for the 50, 75, and 100 mg L^{-1} doses, the required time varied between 50 and 90 min. At the mentioned time points, the residual levels were below 0.1 mg L^{-1} of peroxide. UV reactions with hydrogen peroxide are widely reported in the literature for cyanobacteria removal [25,26] and other applications [27]. Identifying the minimum exposure time required to achieve nearly complete peroxide degradation is essential to eliminate the interference from residual peroxide and ensure the accuracy of AOC quantification in subsequent stages of this study. Therefore, a fixed exposure time of 90 min was set for the peroxide reactions to prevent interference from residual peroxide.

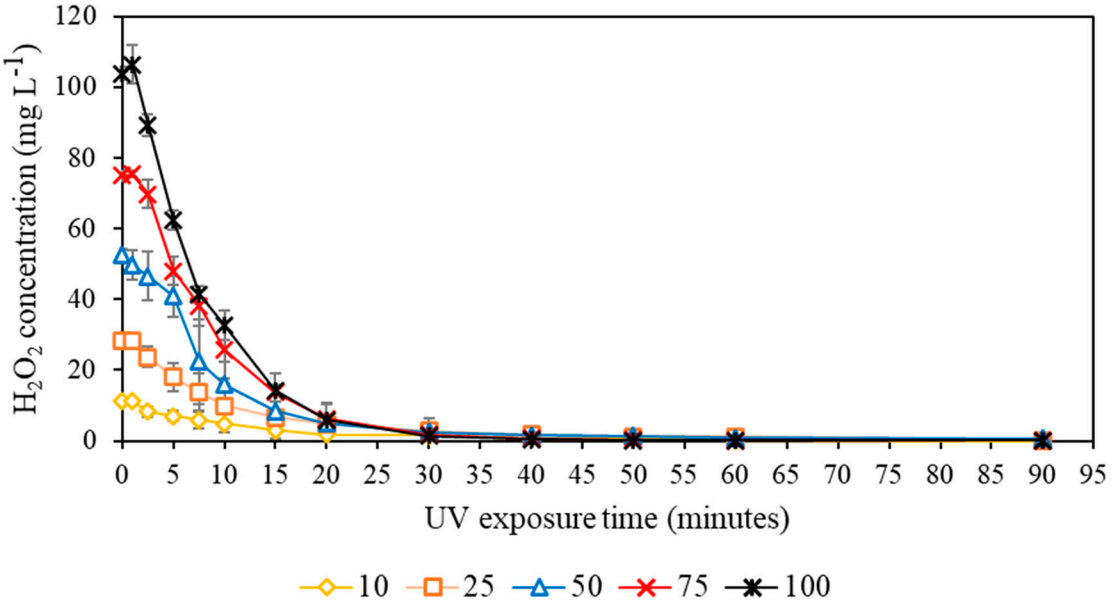


Figure 4. Decomposition curve of H_2O_2 under UV light over 90 min.

3.5. Physicochemical Analysis

3.5.1. Dissolved Organic Carbon (DOC) Analysis

Figure 5 shows the DOC concentration before and after the advanced oxidation process. As indicated by the results, untreated study water exhibited a DOC concentration of approximately 12 mg L^{-1}, corresponding to the cyanobacterial cells in the samples (250,000 cells mL^{-1}). This finding is consistent with previous work [28]. The authors reported that the rise in DOC concentration was associated with the rise in *Microcystis* biomass. After the UV/H_2O_2 process, the DOC concentration gradually decreased. For the 10 mg L^{-1} H_2O_2 dose, the DOC concentration was 10 mg L^{-1}.

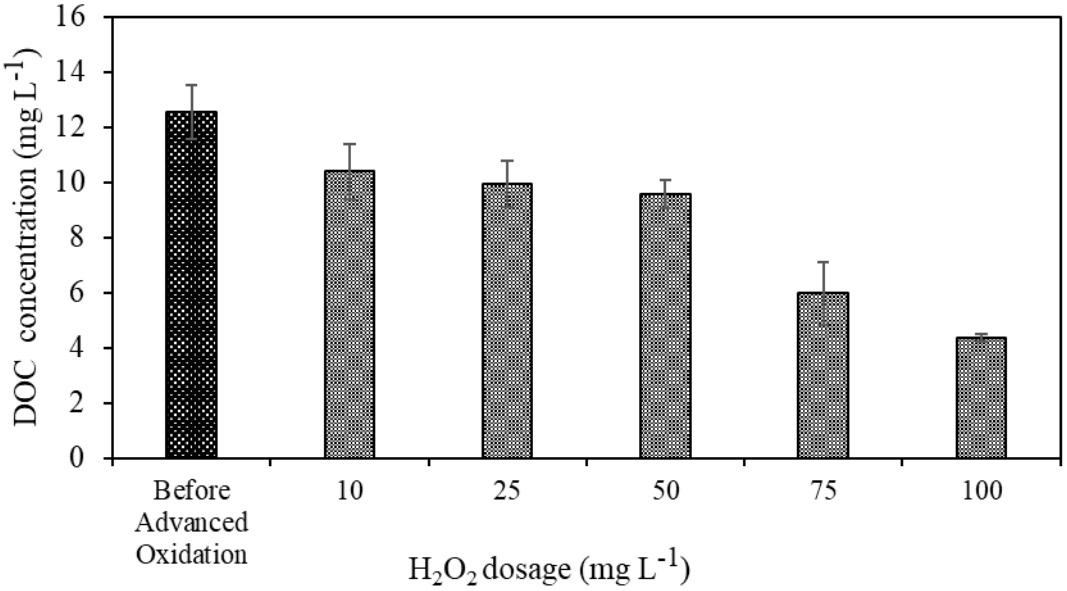


Figure 5. Concentration of DOC before and after UV/H_2O_2 oxidative process (Cell density: 250,000 cells mL^{-1}).

On the other hand, for the 100 mg L^{-1} H_2O_2 dose, the DOC concentration was 4 mg L^{-1}. The higher the oxidant concentration, the greater the reaction rate of hydroxyl radicals and, consequently, the greater the mineralization of DOC. However, high peroxide

doses limit the financial feasibility of applying advanced oxidation processes at a real scale. Additionally, a previous study [29] has reported that the commercial conditions of H_2O_2/UV are insufficient for the complete degradation of natural organic matter. As a result, this organic matter is only partially oxidized, which may lead to an increased formation of disinfection byproducts, such as AOC.

3.5.2. Assimilable Organic Carbon (AOC) Analysis

Figure 6 shows the formation of AOC as a function of peroxide dosages in the UV/H_2O_2 process. The dosage of 10 mg L^{-1} of H_2O_2 presented a higher concentration of AOC (166.7 µgC L^{-1}). A similar result was observed by Bazri and Mohseni [24], reporting a significant increase in the AOC formation in raw waters treated with UV/H_2O_2. The authors attribute this increase to partial oxidation and the fragmentation of larger organic molecules into smaller ones due to reactions with •OH radicals. In contrast, dosages above 50 mg L^{-1} of H_2O_2 reduced the AOC concentration. High dosages of H_2O_2 promote a more complete oxidation of organic matter, leading to the mineralization of the formed AOC. However, as mentioned earlier, high concentrations of H_2O_2 are not always financially viable for large-scale treatment. An alternative is complementing advanced oxidation processes with biological filtration, which helps reduce the AOC levels [21]. Since biologically stable water requires AOC concentrations of up to 50 µgC L^{-1}, only the 50, 75, and 100 mg L^{-1} dosages were able to achieve this stability. These dosages yielded approximate values of 43, 11, and 7 µgC L^{-1} of AOC, respectively. Limiting the concentration of AOC in drinking water is important because these compounds are associated with the growth of heterotrophic bacteria. This growth promotes biofilm formation in distribution systems, posing a challenge to maintaining the microbiological quality of water [30].

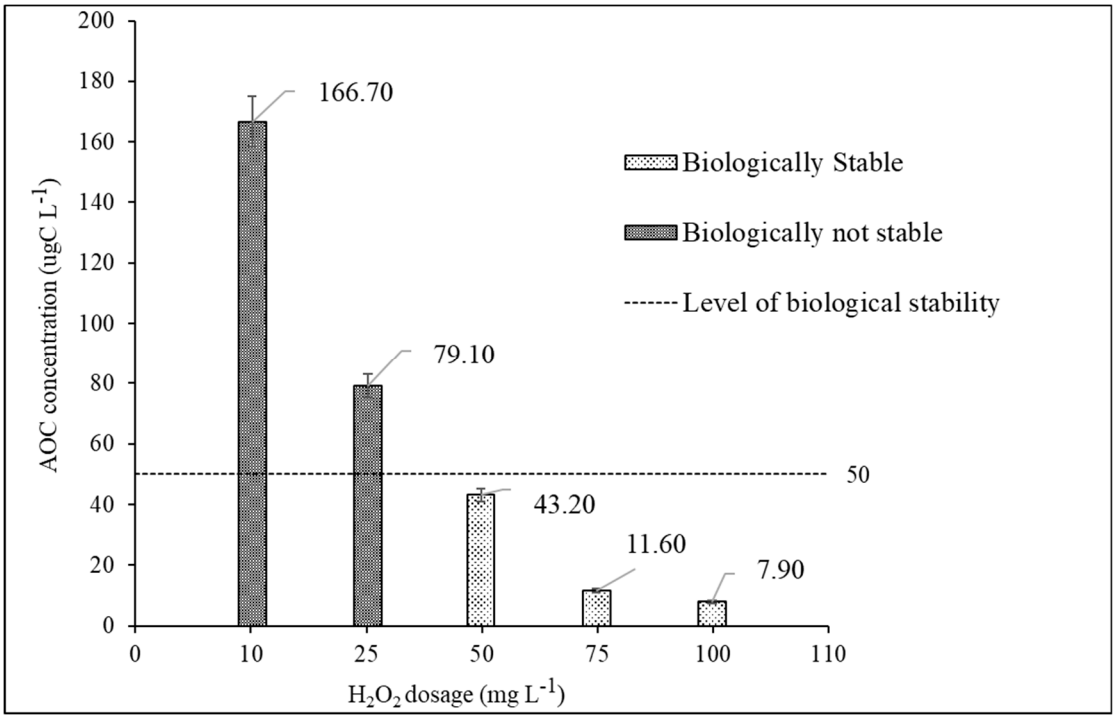


Figure 6. Formation of AOC from the UV/H_2O_2 oxidative process and level of biological stability (Cell density: 250,000 cells mL^{-1}).

3.6. Relation Between AOC and DOC

Figure 7 shows the relationship between AOC and DOC concentrations. AOC and DOC concentrations follow an inversely proportional trend: AOC concentration increases

as the DOC concentration decreases. These results suggest that during the oxidation process, a fraction of DOC was converted into AOC due to the oxidation caused by the UV/H_2O_2 process. The AOC refers to the portion of DOC that is biodegradable and readily utilized by microorganisms. It is estimated that this fraction (AOC) represents between 0.1% and 9.0% of the DOC in drinking water [31,32]. A greater reduction of AOC than DOC was observed for the H_2O_2 dosages between 10 and 50 mg L^{-1}. This can be attributed to a higher tendency for reactions between the OH radicals and AOC.

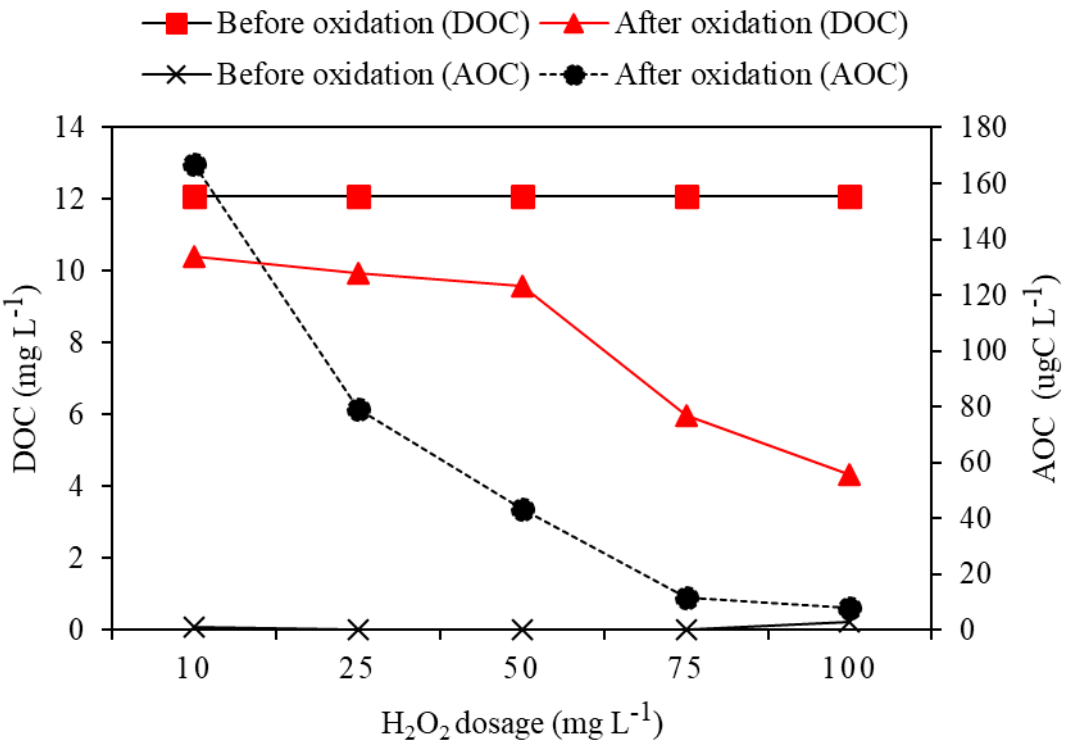


Figure 7. AOC and DOC formation during the UV/H_2O_2 oxidative process (Cell density: 250,000 cells mL^{-1}).

In contrast, for dosages of 75 to 100 mg L^{-1} of H_2O_2, the concentrations of DOC and AOC in the samples are lower. The occurrence of simultaneous reactions between the hydroxyl radicals with AC and DOC can explain this. The excess peroxide in the medium may have led to the transformation of DOC into AOC, resulting in an immediate mineralization of the AOC. As a result, a lower residual AOC is quantified, leading to the samples' lower concentrations of both DOC and AOC simultaneously.

3.7. Trihalomethanes (THMs) Analysis

Figure 8 shows the total THM concentration before and after the UV/H_2O_2 oxidative process. For all dosages, the THM concentration decreases significantly. The concentration decreases from 31 µg L^{-1} to approximately 7 µg L^{-1} for all samples that underwent the UV/H_2O_2 treatment. Mahato et al. (2022) [33] evaluated the reduction of THM precursors using different advanced oxidation processes. The authors identified the Fenton process as the most effective for this removal, attributing its efficiency to the high degradation potential of the hydroxyl radicals generated by this method. Additionally, in this study, it was observed that the studied cell density (250,000 cells mL^{-1}) contributed to 31 µg L^{-1} of the total THMs after chlorination of the samples. A previous study [34] reported increased THMs in waters contaminated with *Microcystis aeruginosa* and *Coccomyxa subellipsoidea* after chlorination.

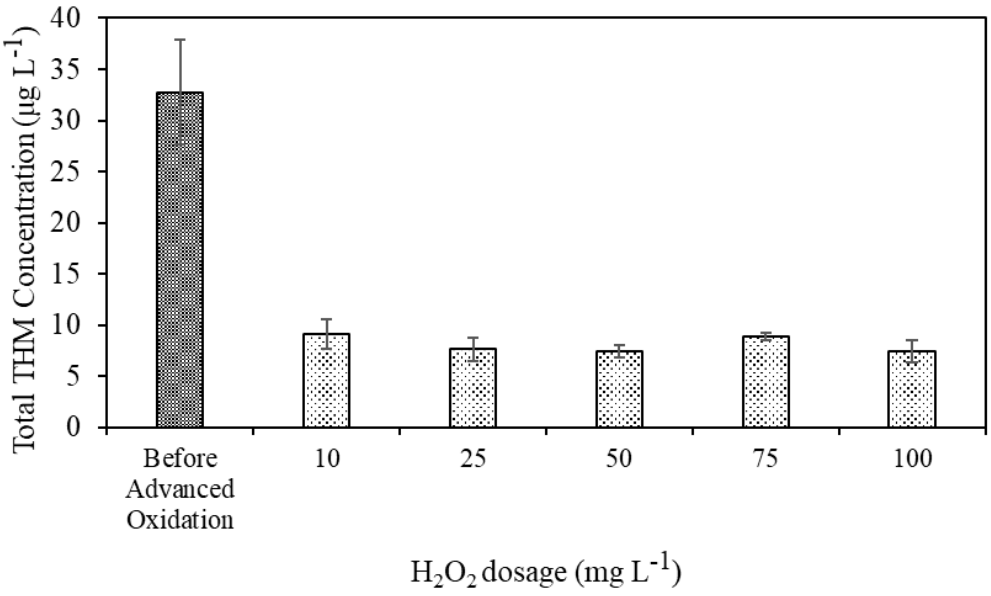


Figure 8. Total THM concentration before and after the UV/H_2O_2 oxidative process (Cell density: 250,000 cells mL^{-1}).

Figure 9 shows the concentrations of the different compounds that make up the group of THMs; these include four distinct compounds: bromoform, dibromochloromethane, bromodichloromethane, and chloroform. In untreated water, the concentration of THMs was predominantly influenced by the formation of chloroform, confirming that cyanobacteria can act as precursors of THMs. This work is consistent with the previous study [35], which reported that chlorination of water containing organic matter derived from cyanobacteria can lead to the formation of chloroform, as observed in the present study. After the UV/H_2O_2 treatment, the concentrations of chloroform and bromodichloromethane were significantly reduced, while that of bromoform showed almost no reduction. According to Medeiros et al. (2019) [36], chloroforms are cytotoxic, whereas dibromochloromethane, bromodichloromethane, and bromoform are mutagenic, genotoxic, and cytotoxic. Examining each of these compounds individually, it becomes clear that the importance of monitoring THMs in drinking water is related to the toxic risk of these molecules.

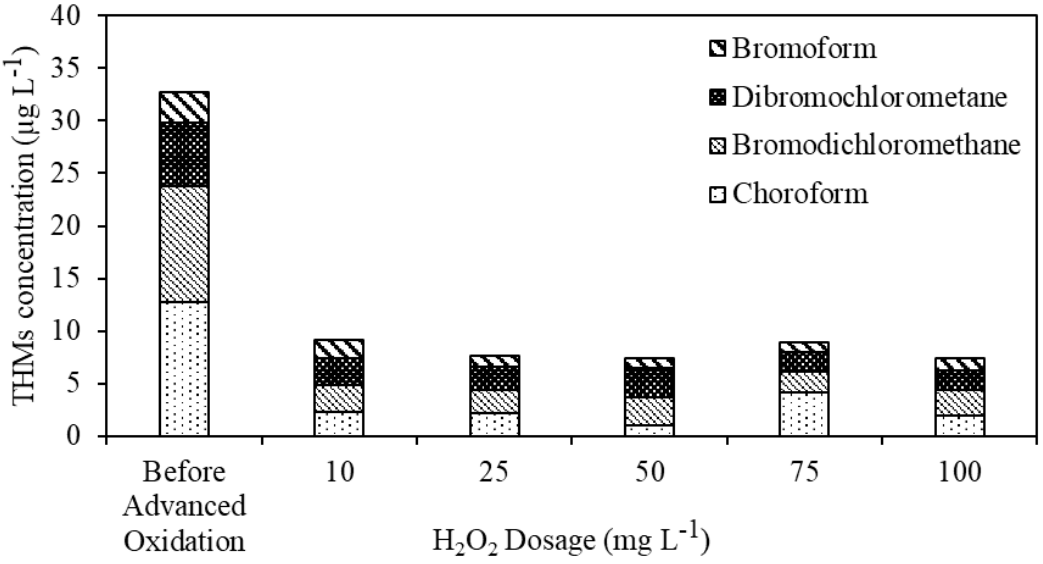


Figure 9. Concentration of trihalomethane compounds before and after UV/H_2O_2 treatment (Cell density: 250,000 cells mL^{-1}).

3.8. Relation Between THMs, DOC, and AOC

Figure 10 shows the relationship between the formation of DOC and the THM concentration after the UV/H_2O_2 process. The concentrations of THMs and DOC decreased after the advanced treatment. However, while the DOC concentration continued to decrease with the increase in H_2O_2 dosage, the formation of THMs was stable in the range of tested H_2O_2 doses from 10 to 100 mg/L. The amount of available, non-degraded organic matter remained constant in all samples, regardless of the H_2O_2 dosage. As a result, THM concentrations were very similar.

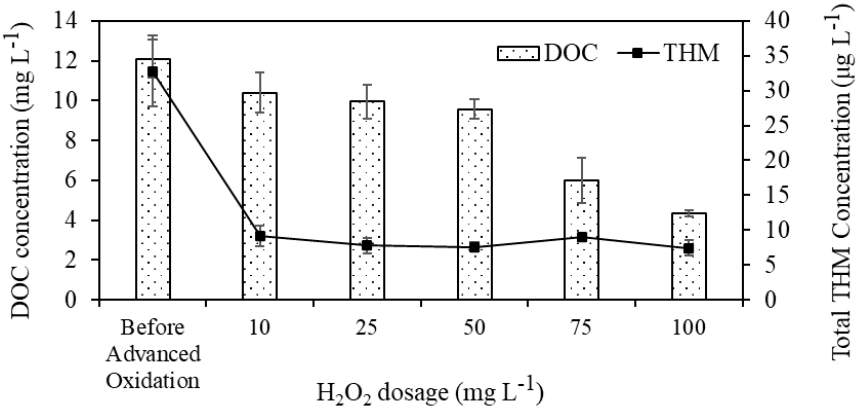


Figure 10. DOC formation related to total THM concentration after UV/H_2O_2 process (Cell density: 250,000 cells mL^{-1}).

Figure 11 shows the relation between the formation of AOC and THMs after the UV/H_2O_2 process. The formation of AOC and THM differed during the oxidation process. The highest AOC concentration was found for a dose of 10 mg L^{-1} H_2O_2 and gradually decreased with higher doses. In contrast, THM formation decreased at 10 mg L^{-1} H_2O_2 and remained constant as the oxidant dosage increased. This indicates that 10 mg L^{-1} of H_2O_2 is sufficient to reduce THMs but not enough to control AOC formation. This increase in AOC formation can be attributed to the partial oxidation of the organic matter from *M. aeruginosa* cells. At higher H_2O_2 doses, the AOC formation decreased, likely because the oxidant was sufficient to mineralize part of the compounds. These results indicate that the formation of AOC and THMs is not directly related to the H_2O_2 conditions and UV exposure time used in this study. This implies that assimilable organic compounds (low molecular weight) do not react with chlorine like other compounds. Consequently, they do not contribute to THM formation.

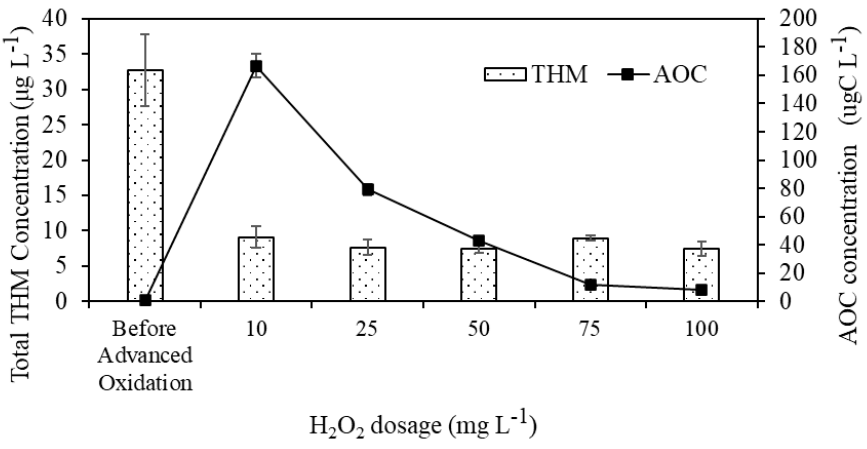


Figure 11. Formation of AOC related to the concentration of total THMs (Cell density: 250,000 cells mL^{-1}).

4. Conclusions

In waters contaminated with cyanobacteria, the formation of AOC can occur when subjected to advanced oxidation treatment (UV/H_2O_2). Under the conditions of this study, AOC and THMs responded differently to oxidation. A decrease in DOC and THM concentrations was observed after the advanced oxidation process, suggesting that the treatment effectively reduced organic matter and minimized the formation of undesirable byproducts. Although the formation of AOC can contribute to the generation of THMs during oxidation, the amount of THMs formed depends on the specific conditions of the disinfection process. The behavior of DOC and AOC were inversely proportional: as the DOC concentration decreased, the AOC concentration increased. This increase in AOC concentration can be attributed to the transformation of the organic matter present in the sample into simpler compounds. This study highlights the importance of understanding the dynamics between the different byproducts formed during advanced oxidation treatment, especially in waters contaminated with cyanobacteria, contributing to optimizing the disinfection processes and minimizing the formation of undesirable byproducts.

Author Contributions: Investigation, L.V.S., F.d.J.B., G.F.S. and L.A.d.A.C.; data curation, L.V.S., R.M.B.R., P.I.M. and F.d.J.B.; writing—original draft, L.V.S., R.M.B.R. and P.I.M.; writing—review and editing, R.M.B.R. and P.I.M.; conceptualization, G.F.S., F.d.J.B. and L.A.d.A.C.; visualization, F.d.J.B. and L.A.d.A.C.; project administration, F.d.J.B. and L.A.d.A.C.; supervision, L.A.d.A.C.; methodology, L.A.d.A.C.; resources, L.A.d.A.C. All authors have read and agreed to the published version of the manuscript.

Funding: The authors would like to thank the National Council for Scientific and Technological Development (CNPq, Process 486789/2013-6) for financial support and scholarships.

Data Availability Statement: The data will be made available from the authors, upon request.

Acknowledgments: FRIOCRUZ: The authors thank the Fiocruz's Technological Platforms Network for use of flow cytometry facility (RPT08L). LAMAQ: The Multi-User Chemical Analysis Laboratory (LAMAQ) - UTFPR for TOC analysis.

Conflicts of Interest: The authors declare no conflicts of interest.

References

1. Kakouei, K.; Kraemer, B.M.; Anneville, O.; Carvalho, L.; Feuchtmayr, H.; Graham, J.L.; Higgins, S.; Pomati, F.; Rudstam, L.G.; Stockwell, J.D.; et al. Phytoplankton and cyanobacteria abundances in mid-21st century lakes depend strongly on future land use and climate projections. *Glob. Chang. Biol.* **2021**, *27*, 6409–6422. [CrossRef] [PubMed]
2. Henderson, R.K.; Baker, A.; Parsons, S.A.; Jefferson, B. Characterisation of algogenic organic matter extracted from cyanobacteria, green algae and diatoms. *Water Res.* **2008**, *42*, 3435–3445. [CrossRef] [PubMed]
3. Fang, J.; Ma, J.; Yang, X.; Shang, C. Formation of carbonaceous and nitrogenous disinfection by-products from the chlorination of Microcystis aeruginosa. *Water Res.* **2010**, *44*, 1934–1940. [CrossRef] [PubMed]
4. Yang, X.; Guo, W.; Shen, Q. Formation of disinfection byproducts from chlor (am) ination of algal organic matter. *J. Hazard. Mater.* **2011**, *197*, 378–388. [CrossRef]
5. Liu, C.; Ersan, M.S.; Plewa, M.J.; Amy, G.; Karanfil, T. Formation of iodinated trihalomethanes and noniodinated disinfection byproducts during chloramination of algal organic matter extracted from Microcystis aeruginosa. *Water Res.* **2019**, *162*, 115–126. [CrossRef]
6. Sriboonnak, S.; Induvesa, P.; Wattanachira, S.; Rakruam, P.; Siyasukh, A.; Pumas, C.; Wongrueng, A.; Khan, E. Trihalomethanes in water supply system and water distribution networks. *Int. J. Environ. Res. Public Health* **2021**, *18*, 9066. [CrossRef]
7. Huang, G.; Ng, T.W.; Chen, H.; Chow, A.T.; Liu, S.; Wong, P.K. Formation of assimilable organic carbon (AOC) during drinking water disinfection: A microbiological prospect of disinfection byproducts. *Environ. Int.* **2020**, *135*, 105389. [CrossRef]
8. Li, W.; Zhang, J.; Wang, F.; Qian, L.; Zhou, Y.; Qi, W.; Chen, J. Effect of disinfectant residual on the interaction between bacterial growth and assimilable organic carbon in a drinking water distribution system. *Chemosphere* **2018**, *202*, 586–597. [CrossRef]

9. Pick, F.C.; Fish, K.E.; Biggs, C.A.; Moses, J.P.; Moore, G.; Boxall, J.B. Application of enhanced assimilable organic carbon method across operational drinking water systems. *PLoS ONE* **2019**, *14*, e0225477. [CrossRef]
10. Yu, H.Y.; Gupta, S.; Zhou, Z. Removal of metals and assimilable organic carbon by activated carbon and reverse osmosis point-of-use water filtration systems. *Chemosphere* **2024**, *365*, 143251. [CrossRef]
11. Ramos, R.M.B.; Paludo, L.C.; Monteiro, P.I.; da Rocha LV, M.; de Moraes, C.V.; Santos, O.O.; Alves, E.R.; Dantas, T.L.P. Amoxicillin degradation by iron photonanocatalyst synthetized by green route using pumpkin (Tetsukabuto) peel extract. *Talanta* **2023**, *260*, 124658. [CrossRef] [PubMed]
12. Sharma, A.; Ahmad, J.; Flora, S.J.S. Application of advanced oxidation processes and toxicity assessment of transformation products. *Environ. Res.* **2018**, *167*, 223–233. [CrossRef] [PubMed]
13. Xu, H.; Zhang, J.; Wang, W.; Li, Y.; Pei, H. Moderate pre-ozonation coupled with a post-peroxone process remove filamentous cyanobacteria and 2-MIB efficiently: From bench to pilot-scale study. *J. Hazard. Mater.* **2022**, *424*, 127530. [CrossRef] [PubMed]
14. Fan, J.; Zeng, J.; Li, X.; Guo, K.; Liu, W.; Fang, J. Multiple roles of UV/$KMnO_4$ in cyanobacteria containing water treatment: Cell inactivation & removal, and microcystin degradation. *J. Hazard. Mater.* **2023**, *457*, 131772. [CrossRef]
15. An, J.; Li, N.; Wang, S.; Liao, C.; Zhou, L.; Li, T.; Wang, X.; Feng, Y. A novel electro-coagulation-Fenton for energy efficient cyanobacteria and cyanotoxins removal without chemical addition. *J. Hazard. Mater.* **2019**, *365*, 650–658. [CrossRef]
16. Gorham, P.R.; Mclachlan, J.; Hammer, U.T.; Kim, W.K. Isolation and culture of toxic strains of Anabaena flos-aquae (lyng) de Breb. *Verh. Int. Verein. Limnol.* **1964**, *15*, 796–804.
17. EPA. *Short-Term Methods for Estimating the Chronic Toxicity of Effluents and Receiving Waters to Freshwater Organisms*; EPA: Washington, DC, USA, 2002.
18. APHA. *Standard Methods for the Examination of Water and Wastewater*; American Public Health Association, American Water Works Association, Water Environment Federation, Eds.; American Public Health Association: Washington, DC, USA, 2005.
19. Hammes, F.A.; Egli, T. New method for assimilable organic carbon determination using flow-cytometric enumeration and a natural microbial consortium as inoculum. *Environ. Sci. Technol.* **2005**, *39*, 3289–3294. [CrossRef]
20. Hammes, F.; Egli, T. *A Flow Cytometric Method for COA Determination*; Techneau: Marigny-le-Lozon, France, 2007; Volume 6, 16p.
21. Hammes, F.; Salhi, E.; Köster, O.; Kaiser, H.P.; Egli, T.; Von Gunten, U. Mechanistic and kinetic evaluation of organic disinfection by-product and assimilable organic carbon (AOC) formation during the ozonation of drinking water. *Water Res.* **2006**, *40*, 2275–2286. [CrossRef]
22. Klassen, N.V.; Marchington, D.; McGowan, H.C. H_2O_2 determination by the I3-method and by $KMnO_4$ titration. *Anal. Chem.* **1994**, *66*, 2921–2925. [CrossRef]
23. Bazri, M.M. Assimilable Organic Carbon Formation During Ultraviolet-Hydrogen Peroxide Advanced Oxidation Treatment of Surface Water. Doctoral Dissertation, University of British Columbia, Vancouver, BC, Canada, 2010. [CrossRef]
24. Bazri, M.; Mohseni, M. Pretreatment of natural organic matter to control biological stability. *Environ. Sci. Water Res. Technol.* **2016**, *2*, 298–303. [CrossRef]
25. Yan, B.; Wang, S.; Liu, Z.; Wang, D.; Shi, W.; Cui, F. Degradation mechanisms of cyanobacteria neurotoxin β-N-methylamino-l-alanine (BMAA) during UV254/H_2O_2 process: Kinetics and pathways. *Chemosphere* **2022**, *302*, 134939. [CrossRef] [PubMed]
26. Wang, B.; Wang, X.; Hu, Y.; Chang, M.; Bi, Y.; Hu, Z. The combined effects of UV-C radiation and H_2O_2 on Microcystis aeruginosa, a bloom-forming cyanobacterium. *Chemosphere* **2015**, *141*, 34–43. [CrossRef] [PubMed]
27. Pratiwi, W.Z.; Hadiyanto, H.; Widayat, W. Response surface optimization of UV/H_2O_2-based photo-oxidative degradation of amoxicillin. *Results Eng.* **2024**, *21*, 101836. [CrossRef]
28. Hu, L.; Shan, K.; Huang, L.; Li, Y.; Zhao, L.; Zhou, Q.; Song, L. Environmental factors associated with cyanobacterial assemblages in a mesotrophic subtropical plateau lake: A focus on bloom toxicity. *Sci. Total Environ.* **2021**, *777*, 146052. [CrossRef]
29. Sarathy, S.R.; Mohseni, M. The impact of UV/H_2O_2 advanced oxidation on molecular size distribution of chromophoric natural organic matter. *Environ. Sci. Technol.* **2007**, *41*, 8315–8320. [CrossRef]
30. Van der Kooij, D.; Hijnen WA, M.; Kruithof, J.C. The effects of ozonation, biological filtration and distribution on the concentration of easily assimilable organic carbon (AOC) in drinking water. *Ozone Sci. Eng.* **1989**, *11*, 297–311. [CrossRef]
31. Escobar, I.C.; Randall, A.A. Assimilable organic carbon (AOC) and biodegradable dissolved organic carbon (BDOC): Complementary measurements. *Water Res.* **2001**, *35*, 4444–4454. [CrossRef]
32. Westphalen AP, C.; Corção, G.; Benetti, A.D. Utilização de carvão ativado biológico para o tratamento de água para consumo humano. *Eng. Sanit. E Ambient.* **2016**, *21*, 425–436. [CrossRef]
33. Mahato, J.K.; Gupta, S.K. Advanced oxidation of Trihalomethane (THMs) precursors and season-wise multi-pathway human carcinogenic risk assessment in Indian drinking water supplies. *Process Saf. Environ. Prot.* **2022**, *159*, 996–1007. [CrossRef]
34. Ma, M.; Wang, M.; Cao, X.; Li, Y.; Gu, J. Yield of trihalomethane, haloacetic acid and chloral upon chlorinating algae after coagulation-filtration: Is pre-oxidation necessarily negative for disinfection by-product control? *J. Hazard. Mater.* **2019**, *364*, 762–769. [CrossRef]

35. Morris, J.C.; Baum, B. Precursors and mechanisms of haloformations in the chlorination of water supplies. In *Relative Dominance of Haloacetic Acids and Trihalomethanes in Treated Drinking Water*; AWWA, Research Fundation: Denver, CO, USA, 2002; ISBN 1-58321-117-9.
36. de Castro Medeiros, L.; de Alencar FL, S.; Navoni, J.A.; de Araujo AL, C.; do Amaral, V.S. Toxicological aspects of trihalomethanes: A systematic review. *Environ. Sci. Pollut. Res.* **2019**, *26*, 5316–5332. [CrossRef]

Disclaimer/Publisher's Note: The statements, opinions and data contained in all publications are solely those of the individual author(s) and contributor(s) and not of MDPI and/or the editor(s). MDPI and/or the editor(s) disclaim responsibility for any injury to people or property resulting from any ideas, methods, instructions or products referred to in the content.